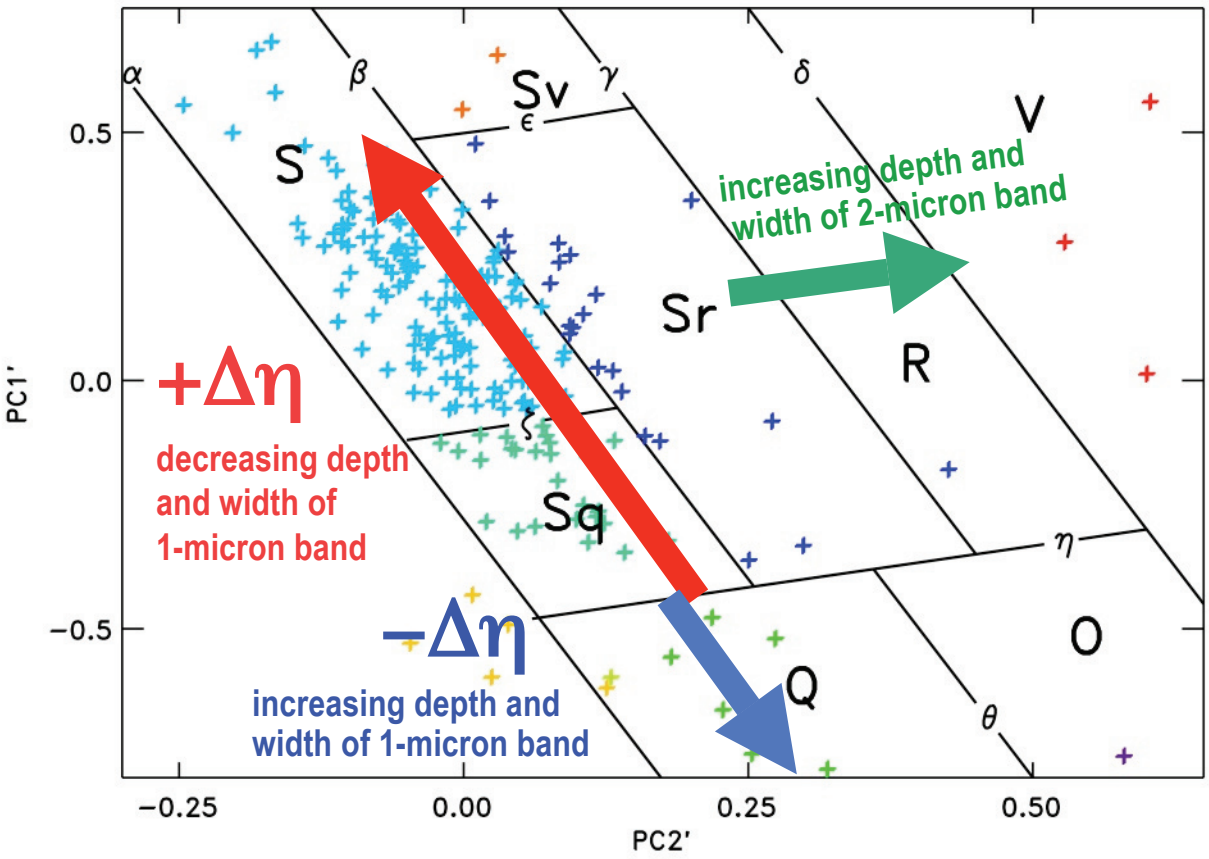

Supplementary Figure 1. Spectral trends within principal component space of the Bus-DeMeo[10] taxonomy. The first two principal components PC1' and PC2' are computed after the removal of spectral slope. Regions bounding the taxonomic classes are then defined[10] within this slope-free space of PC1' versus PC2'. The boundary between Sq- and Q-types is determined by line η. The definition of line η was chosen[10] so as to occur at a natural break in the trends of available data and to be most fully consistent with objects defined as Q-types in the Bus[31] taxonomy. The sign and value of the parameter Δη denotes the perpendicular distance above or below line η. (This figure adapted from Figure 3 of DeMeo et al. 2009.)[10]

The Sample

The Mars-crossing and near-Earth asteroids in our sample are defined as those coming inside the orbit of Mars and within 0.3 astronomical units (AU) from the Earth, respectively (1 AU is the Earth-Sun distance); are remnants from our Solar System's formation that predominantly come from the main asteroid belt between Mars and Jupiter. As such, they are an observable link (large enough for current techniques to discover and track; typically 100m to ~10 km across) to the flux of meteorites from the asteroid belt. We have been conducting an ongoing survey[29] with routine measurement techniques[24] of the near-infrared (0.8- to 2.5-micron) reflected spectral colours of Earth- and Mars-crossing asteroids using the 3m aperture NASA Infrared Telescope Facility (IRTF) located on Mauna Kea, Hawaii, accumulating a sample of more than 300 objects over an interval of 9 years.

Supplementary Table 1

We present a tabulation of our sample of 95 Mars-crossing (MC) and near-Earth asteroids. For the latter, we indicate their orbital properties based on their semi-major axes (a), perihelion distances (q), and aphelion distances (Q). Amors (AMO) have 1.017 AU < q ≤ 1.3 AU; Apollos (APO) have a ≥ 1 AU, q ≤ 1.017 AU; Atens (ATE) have a < 1 AU, Q > 0.983 AU. The H magnitude is the mathematical value for the apparent brightness of the asteroid if placed at the hypothetical position 1 AU from the Earth, 1 AU from the Sun, with a solar phase angle of zero degrees. As a close approximation, an H magnitude of 17.5 corresponds to a diameter of 1 km for a typical debiased albedo[20] of 0.24 for the S-, Sq- and Q-type objects tabulated. Supplementary Table 1 presents all S-, Sq-, and Q-type asteroids from our survey that fall within the H magnitude range of the subset of Q-types. In other words, our Q-type subset has an H magnitude range of 14.0 to 20.8. Therefore only S- and Sq-types in this same range are included in our tabulation and our analysis. (We have many additional surveyed near-Earth asteroids outside of this H magnitude range, but they are excluded so as to minimize any possible bias effects that may be introduced by comparing asteroids over different size ranges.)

The fourth column of Supplementary Table 1 provides the classification within the Bus-DeMeo taxonomy[10]. We note that the notation "w" is not a class, rather indicates objects having higher slopes within that class. We describe in greater detail below (see Supplementary Notes section) that spectral slope is removed prior to the computation of principal component scores and assignment to the S-, Sq-, Q-type classes. Spectral slope has no role in our analysis.

The fifth column of Supplementary Table 1 provides the current value of the Minimum Orbit Intersection Distance (MOID), as described in the main text. As the

main text also describes, for each object we integrate its orbit backward in time for -500,000 years, beginning with the current epoch, recording the value of the MOID at 50 year intervals. This creates a set of 10,000 MOID values for each object, which when added with the six clones (see main text), each object in the table has 70,000 calculated values for its MOID that explore its orbital history over the past 500,000 years. In the last column, we tabulate for each object the lowest value found among all 70,000 orbital integrations. We emphasize these are simply snapshots of the minimum possible encounter distance between the Earth and the object, but they do not give any information on whether or not an encounter at this distance actually occurred.

Supplementary Table 1

Number	Name / Designation	Orbit Description	H Magnitude	Bus-DeMeo Taxonomy	Current MOID (AU)	Lowest Value MOID (AU)
Objects with MOID values entering inside the Lunar Distance						
719	Albert	AMO	15.8	S	0.18218	0.000464
1566	Icarus	APO	16.0	Q	0.03468	0.000052
1620	Geographos	APO	15.6	S	0.03015	< 0.000043
1685	Toro	APO	14.2	Sq	0.05075	< 0.000043
1862	Apollo	APO	16.2	Q	0.02591	< 0.000043
1864	Daedalus	APO	14.9	Sq	0.26840	< 0.000043
1865	Cerberus	APO	17.0	S	0.15591	< 0.000043
1943	Anteros	AMO	15.8	Sw	0.06269	< 0.000043
2063	Bacchus	APO	17.1	Sq	0.06742	< 0.000043
3288	Seleucus	AMO	15.3	Sw	0.09942	< 0.000043
3753	Cruithne	ATE	15.6	Q	0.07146	< 0.000043
4179	Toutatis	APO	15.3	Sq	0.00608	< 0.000043
4197	1982 TA	APO	14.6	Sq	0.09431	< 0.000043
4544	Xanthus	APO	17.1	Sq,S	0.17386	< 0.000043
4688	1980 WF	AMO	19.0	Q	0.11130	< 0.000043
5011	Ptah	APO	17.1	Q	0.02476	< 0.000043
5143	Heracles	APO	14.0	Q	0.06102	< 0.000043
5660	1974 MA	APO	15.7	Q	0.16002	0.000053
5693	1993 EA	APO	16.8	Sq,S	0.00556	< 0.000043
5786	Talos	APO	17.0	S,Sq	0.18924	< 0.000043
6047	1991 TB1	APO	17.0	S	0.14006	< 0.000043
6239	Minos	APO	17.9	Sqw	0.02640	< 0.000043
7341	1991 VK	APO	16.7	Q	0.04825	< 0.000043
18736	1998 NU	AMO	16.1	Sw	0.22030	0.000065
19356	1997 GH3	AMO	17.1	Sq	0.08885	< 0.000043
20429	1998 YN1	APO	18.0	Sq	0.05622	< 0.000043
20790	2000 SE45	AMO	16.6	S	0.22192	0.000064
22753	1998 WT	APO	17.7	Sq	0.03347	< 0.000043
22771	1999 CU3	APO	16.8	S	0.06311	0.000055
23187	2000 PN9	APO	16.1	Sq	0.01560	< 0.000043
31669	1999 JT6	APO	16.0	Sqw	0.00354	< 0.000043
35107	1991 VH	APO	16.9	Sq	0.02650	< 0.000043
52340	1992 SY	APO	18.1	Q	0.09736	< 0.000043
66063	1998 RO1	ATE	18.0	S	0.09151	< 0.000043
66146	1998 TU3	ATE	14.5	Q	0.07327	< 0.000043
85713	1998 SS49	APO	15.8	S	0.00323	< 0.000043
85770	1998 UP1	ATE	20.5	Sq	0.08336	< 0.000043
86039	1999 NC43	APO	16.0	Sq	0.02432	< 0.000043
86819	2000 GK137	APO	17.4	Sq	0.01558	< 0.000043
87024	2000 JS66	APO	18.7	Sq	0.09652	< 0.000043
87684	2000 SY2	ATE	16.4	Q	0.04631	< 0.000043
90403	2003 YE45	APO	17.8	Sq	0.03644	< 0.000043
98943	2001 CC21	APO	18.5	Sw	0.08306	< 0.000043
99942	Apophis	ATE	19.2	Sq	0.00017	< 0.000043
138258	2000 GD2	ATE	19.1	Sq	0.07165	< 0.000043
139622	2001 QQ142	APO	18.4	Sq	0.01067	< 0.000043
142348	2002 RX211	AMO	18.1	S,Sq	0.14493	< 0.000043
144900	2004 VG64	ATE	18.3	Sq	0.02790	< 0.000043
152895	2000 CQ101	AMO	18.1	Sq,S	0.15443	< 0.000043
162058	1997 AE12	AMO	17.8	Q	0.09049	0.000050
162781	2000 XL44	AMO	17.7	S	0.29571	< 0.000043
184266	2004 VW14	APO	19.4	Q	0.01068	< 0.000043
200840	2001 XN254	APO	17.6	S	0.03879	< 0.000043
	2000 CH59	ATE	19.6	Sq	0.02332	< 0.000043
	2000 GF2	APO	20.5	S	0.01087	< 0.000043
	2000 QW7	AMO	19.8	Q	0.02930	< 0.000043
	2001 BE10	ATE	18.9	Sq	0.04108	< 0.000043
	2001 FA1	AMO	17.7	Sq	0.25561	< 0.000043
	2002 AA	APO	19.3	S	0.05757	< 0.000043
	2002 GO5	APO	18.6	Sq	0.03474	0.000086
	2002 NY40	APO	19.3	Q	0.00108	< 0.000043
	2004 TP1	APO	20.7	Sq	0.02741	< 0.000043
	2005 ED318	AMO	20.8	Q	0.00984	< 0.000043
	2005 ND7	AMO	16.5	S	0.19066	0.000048
	2006 BN55	APO	19.8	Sq	0.05624	< 0.000043
	2006 NM	AMO	16.3	Sq,S	0.09172	0.000064
	2006 UL217	APO	20.7	Sq	0.02097	< 0.000043
	2006 VB14	ATE	18.5	Q	0.07769	< 0.000043
	2006 VQ13	APO	20.1	Sq	0.00831	< 0.000043
	2006 VV2	APO	16.7	S	0.01372	0.000048
	2007 DT103	APO	19.2	Q	0.01444	< 0.000043
	2007 LL	ATE	20.3	Q	0.08468	< 0.000043
	2007 RF5	APO	18.4	Sq	0.20847	< 0.000043
	2008 CL1	ATE	19.5	Q	0.10065	< 0.000043
	2008 DE	APO	19.7	Sq	0.00528	< 0.000043
Objects with MOID values remaining outside the Lunar Distance						
1198	Atlantis	MC	14.6	Sw	0.49080	0.457277
1916	Boreas	AMO	14.9	Sw	0.25310	0.197087
2074	Shoemaker	MC	14.0	Sw	0.66704	0.523022
3102	Krok	AMO	15.6	Sqw	0.18536	0.095134
3122	Florence	AMO	14.2	Sqw	0.04390	0.037381
3198	Wallonia	MC	16.8	Sqw	0.70952	0.648695
6585	O'Keefe	MC	14.3	S	0.62507	0.623009
24475	2000 VN2	AMO	16.3	Sw	0.14996	0.098065
47581	2000 AN178	MC	15.1	Sqw	0.61363	0.131421
54690	2001 EB	AMO	17.1	S	0.41249	0.327926
65784	1995 UF4	MC	15.2	Sq	0.59669	0.542772
86212	1999 TG21	MC	14.5	S	0.65129	0.597647
86324	1999 WA2	AMO	15.7	S	0.34159	0.250320
136993	1998 ST49	APO	17.7	S	0.06036	0.029255
144922	2005 CK38	AMO	17.3	Sq	0.25876	0.074269
162181	1999 LF6	APO	18.1	S	0.06332	0.047817
	2000 OG8	AMO	17.8	S	0.23821	0.118132
	2000 SL	APO	18.5	S	0.12456	0.043919
	2005 QE166	AMO	17.0	S	0.36489	0.064107
	2006 UM	AMO	18.5	Sq	0.15001	0.054348

Notes

Unlike previous analyses of possible orbital[6] or size-dependent[4] trends for near-Earth S-, Sq-, and Q-types, our analysis is not based on spectral slope. The reason our analysis is different (and hence independent of spectral slope) is the reliance on all spectral quantification using the Bus-DeMeo taxonomy[10]: Slope is removed as the first step in the Bus-DeMeo taxonomy. With the slope removed, the principal component scores are calculated. The first two principal components, which are independent of slope, are denoted as PC1' and PC2'. Assignment of asteroids into the S-, Sq-, and Q-type classes is based on the calculated values of the first two principal components, PC1' and PC2'. (See Supplementary Figure 1.)

If spectral slope is not a factor, what is the distinction of S-, Sq-, and Q-type asteroids within the Bus-DeMeo taxonomy[10]? As those authors note, PC1' and PC2' are sensitive to the depth and width of the 1- and 2-micron absorption bands. Referring to their[10] Figure 3 (adapted here as Supplementary Figure 1): moving downward and parallel to lines α and β, increases the depth and width of the 1-micron absorption band. PC1' and PC2' scores falling below line η are "Q-types". The "spectral parameter" plotted along the vertical axis in Figure 2 of the main manuscript measures the perpendicular distance from line η. Denoting this perpendicular distance as $\Delta\eta$, it is calculated[10] by:

$$\Delta\eta = \frac{-\frac{1}{3}PC2' + PC1' + 0.50}{1.0541}$$

Q-types reside below line η and have negative $\Delta\eta$ values while Sq- and S-types reside above line η and have increasingly positive $\Delta\eta$ values. Thus the change in spectral properties from Q-types, to Sq-types, to S-types (in other words, larger positive values for $\Delta\eta$) correspond spectrally to a decrease in the depth and width of the 1-micron absorption band. Such spectral alterations are consistent with the type of spectral weathering effects seen for solar wind ion implantation models[28].

If spectral slope is not a factor considered within our analysis, then what are possible alternative explanations for "slope trends" previously analyzed[4,6] for near-Earth S-, Sq-, and Q-types? For the dependence of spectral slope with respect to size[4], those

authors present two alternatives: a) Younger surface ages due to younger collisional ages at smaller sizes; b) spectral or weathering effects that are dependent upon the surface gravity (and hence size) necessary for the development and retention of regolith. Those authors[4] note that if space weathering timescales prove to be very rapid, then alternative (b) is to be favored. Vernazza et al.[3] and our current results strongly support the rapid rate of space weathering, therefore pointing to their[4] alternative (gravity dependence) explanation rather than a collisional / weathering age.

For the dependence of spectral slope with respect to orbits[6], we note a bias for the discovery of smaller objects in the very near vicinity of Earth – thereby allowing the same size-dependent slope effects noted above, if they are indeed relevant, to be part of the observed trend. However we note that even the planet crossing hypothesis, by itself, can introduce some possible size-dependent effects: Large objects (multi-km) pass much less frequently in the Earth's vicinity, making their tidal resurfacing timescales longer than the "fast" space weathering timescale.

Finally we address a common misconception that ordinary chondrite compositions can only be found for asteroids having Q-type taxonomy classifications. Recognition that ordinary chondrite compositions are possible among asteroids displaying S-type spectra has been long standing, most quantitatively addressed by Gaffey et al.[30] and more historically addressed by Gaffey et al.[26] As noted in the main text, the Near-Earth Asteroid Rendezvous mission brought *in situ* confirmation that the S-type asteroid Eros has elemental abundance measurements[22] consistent with an ordinary chondrite composition. Eros is interpreted as having an ordinary chondrite composition with a “space weathered” surface spectrum.

References Cited in Supplementary Information

[29]Binzel, R. P., Rivkin, A. S., Thomas, C. A., DeMeo, F. E., Tokunaga, A. & Bus, S. J. The MIT-Hawaii-IRTF Joint Campaign for NEO Spectral Reconnaissance. *LPSC XXXVI*, Abstract 36.1817 (2005).

[30]Gaffey M. J., Bell J. F., Brown R. H., Burbine T. H., Piatek J. L., Reed K. L. and Chaky D. A. Mineralogical variations within the S-type asteroid class. *Icarus* **106**, 573-602 (1993).

[31]Bus, S.J., and Binzel, R.P., Phase II of the Small Main-Belt Asteroid Spectroscopic Survey: A feature-based taxonomy. *Icarus* **158**, 146-177 (2002).